



A study of the evolution of the particle boundary layer in a reservoir, using laser particle sizing

Xavier Casamitjana*, Teresa Serra, Mariana Soler, Jordi Colomer

Physics Department, Universitat de Girona, E.P.S., Campus de Montilivi, Girona17071, Spain

Received 9 October 2001; received in revised form 15 March 2002; accepted 12 April 2002

Abstract

The dynamics of the particle boundary layer in the Boadella reservoir was studied using an in situ laser optical particle-sizing instrument. This layer was found at the bottom of the reservoir from summer until the end of the year, when the reservoir was fully mixed. Most of the particles in this layer are remnants of the summer algae bloom and are trapped in the boundary layer due to the thermal stratification. The phytoplankton bloom is mainly composed of diatoms, with diameter $d \sim 5 \mu\text{m}$ and green algae with diameter $d \sim 15 \mu\text{m}$. Inorganic particles and decomposed organic particles with $d < 3 \mu\text{m}$ are also encountered in the boundary layer. On the other hand, particles with diameter between 30 and 100 μm are mostly found in the epilimnion of the reservoir. These are a mixture of aggregates of inorganic particles, colonies of phytoplankton, zooplankton, detritus, etc. Different mixing events occurring during autumn resuspended the small particles in the boundary layer, while the greater particles settled down. The extent of the resuspension has been parameterized with a non-dimensional number that balances the stress across the interface and the strength of the stratification. © 2002 Elsevier Science Ltd. All rights reserved.

Keywords: Limnology; Suspended sediments; Laser diffraction; Particle sizes; Particle resuspension; Water quality

1. Introduction

In studying the ecology of lakes, it is important to find out when the turbulent activity in the benthic boundary layer becomes strong enough to resuspend the sediments [1]. In the boundary layer, particles are maintained in suspension because the upward diffusion of sediment is balanced by the downward settling of particles. Agrawal and Traykovski [2] examined the dynamics of a particle size distribution in a marine bottom boundary layer that was subjected to enhanced stresses produced by currents and waves. They found that, despite a decrease in optical transmission that would normally be interpreted as an increasing sediment load, a dramatic decrease in suspended particle sizes revealed an actual reduction in suspended

volume. Compared to the ocean, enclosed water bodies, like lakes or reservoirs allow us to study the phenomenology and dynamics of the boundary layers under much more controlled conditions. Gloor et al. [3] compared the mixing process in the bottom boundary layer of lakes with sloping boundaries, with the mixing in lakes with a flat bottom. They used microstructure measurements to show that the mixing over the sloping boundaries is considerably more efficient. MacIntyre et al. [4] found that the inshore eddy diffusivity values at 4 m from the bottom were two to four orders of magnitude greater than they were offshore at the same depths. Also Wieland et al. [5] found lateral sediment transport, which caused an increase in the sedimentation rates, accumulating and forming a patchy, nepheloid layer in the slightly denser bottom waters which contained more fine-grained particles in suspension.

Although the measurement of the particle concentration in lakes, or in marine environments, is an important

*Corresponding author. Fax: +34-972-41-80-98.

E-mail address: xavier.casamitjana@udg.es
(X. Casamitjana).

parameter to estimate the water quality, there are only a few studies where the particle concentration is directly measured. Dickey et al. [6] provide a unique set of physical and optical observations in a marine environment during the passage of two hurricanes. Mikkelsen and Pejrup [7] used averaged values of the particle concentration, measured with the in situ particle sizer LISST-100, together with the total suspended matter to calculate the difference in density between the flocculated suspension and the ambient water. Granata et al. [8] mapped the time series of currents, wave velocities and particle concentrations to give a picture of the fine-scale processes in a sea-grass meadow. They found high particle number concentration (PNC) values under high levels of turbulence above the barren sand area and inside the meadow, whereas at low levels of turbulence, small particles were only resuspended above the barren sand area but not within the meadow. Other systems, such as submersible cameras, have been used previously to determine, in situ, the particle concentration in natural systems [9,10]. Unfortunately, submersible cameras do not provide measurements of particles with diameter $<20\mu\text{m}$ and are not capable of counting a large population of particles. Therefore submersible cameras cannot be used to make good estimations of the particle concentration.

In the past years, suspended sediment concentration has been estimated using one parameter only: optical transmission, optical backscatter or acoustic scattering cross section. For example, Ridd et al. [11] measured the siltation of sediment by using an optical fiber backscatter. For big particles, such as marine snow, a typical method for measuring particle sizes has involved the use of a camera system followed by image processing and data analysis [12]. Another common parameter measured in lakes is particle deposition, using sediment traps. For example Wieland et al. [5] measured the particle fluxes in lower Lake Zurich, by using a two-dimensional array of sediment traps. To estimate a multi-valued size distribution, a multi-parameter sensor must obviously be employed. Laser diffraction instruments have been used in laboratories to measure particle size distribution for at least the last two decades. Bale and Morris [13] developed the first underwater instrument based on this technique. They adapted a commercial laboratory instrument, manufactured by Malvern Instruments of the UK, for ocean use. In this paper, we describe how the LISST-100 instrument, developed by Agrawal and Pottsmith [14], was used to study the dynamics of a particle boundary layer in Boadella reservoir. The LISST-100 (laser in situ scattering and transmissometry probe), unlike those of Bale and Morris [13], is autonomous, battery-powered and equipped with a computer and memory for data storage.

2. Methods

The study presented here was carried out in Boadella reservoir. This reservoir is located in the north-east of Spain in the eastern pre-Pyrenees ($42^{\circ}20.3\text{N}$ $2^{\circ}21.1\text{E}$). It has a maximum capacity of 62hm^3 and a maximum surface area of 364ha . Maximum elevation is 160m ASL (above sea level) and its base is at 106m ASL. Outflow spills are located at 127 and 116m , ASL. The lake's hydrological regime, as with most of the lakes in the Mediterranean area, mainly depends on the seasonal nature of rainfall events. High rainfall is commonly associated with storm-fronts in spring and fall, and relatively low rainfall occurs in summer and winter.

The LISST-100 determines the size distribution of an ensemble of particles from their characteristic multi-angle forward scattering. The multi-angle measurements are at small forward angles, from 0.05° to 5° . At these small angles, the particle scattering is independent of both the particle refractive index and the composition of the particles and depends only on the particle size. The instrument emits a collimated laser beam that produces the scattering of the particles. The scattered light is focussed by means of a lens in a "ring detector" placed in the focal plane of the lens. All rays originating at a particular angle to the optical axis arrive at the detector at a point in the focal plane that lies at the same angle from the lens axis. The detector is formed by 32 concentric rings of silicon and each ring responds to the scattering integrated over a narrow range of angles. The measured diffracted energy in the rings is related to the area distribution of the particles by means of a kernel matrix that has to be inverted in order to obtain the area distribution of the particles. The volume distribution is then computed from the area distribution by multiplication of the area in each size bin with its mean diameter. The LISST-100 instrument employed in the experiment described in this paper measured size distributions over the size range $1.2\text{--}200\mu\text{m}$. Also, a Chl *a* (Minitracka II, Chelsea Instruments, UK), with a resolution of $0.01\mu\text{g/L}$, was linked to the LISST-100 as an external sensor.

We used the LISST-100 in two different ways. Firstly, the instrument was deployed monthly, from June to November 2000, to measure the particle distribution and the Chl *a* concentration in the water column. Measurements were made at depth-intervals of $0.5\text{--}1\text{m}$ from the surface of the lake to the bottom. To avoid possible vertical displacements due to the boat movements, ten consecutive measurements were made at each depth, and averaged. The particle size results were integrated in order to obtain the PNC and the particle volume concentration (PVC). The in situ profiles were checked to detect peaks of PVC and Chl *a* concentration. Also, water samples were taken at depths where peaks of PVC were detected, in order to identify phytoplankton

populations. Water samples were collected using a double-ended, cone shaped device, specially designed to avoid shear stresses on organisms and inorganic populations when pumped from the selected depth to the surface [15]. These samples were fixed in the field with formaldehyde (4%) and stored in a fridge at 4°C until they were measured. Samples were filtered in the laboratory for later identification of particles under an electron microscope.

Secondly, the LISST-100 was deployed in a continuous mode from 28 September until 17 October 2000. For this work the instrument was moored at 8 m above the bottom, in the deepest area of the reservoir. Five samples per second were taken and averaged over a 3 s period, at intervals of 50 s; this procedure was repeated 12 times; then the instrument stopped sampling for 50 min. Details regarding the measurement technique and analysis of raw data can be found in Agrawal and Pottsmith [14]. Unfortunately, the fouling of the optical windows affected the measurements taken with LISST-100, due to the long period that the instrument was deployed in the water. This is a common problem with all optical sensors, when deployed in natural waters. Agrawal and Traykovsky [2] suggested changing the background light scattering level. Normally, the background scattering level is calibrated with filtered water. When there is clear evidence of fouling, one can try to estimate the particle sizes by assuming that the scans with the lowest energy in the rings can be used for background light scattering level. Our data suggest that, when the LISST-100 works in a continuous mode, fouling of the optical windows affected the small scan angles, which correspond to the largest particles. The response to the smallest particles seemed or not to be affected by fouling, or affected in small extent. This can be deduced by looking at the scattering patterns. Also, when discrete profiles were taken, the deduced PVC for the smallest particles ($d < 10 \mu\text{m}$) agreed with PVC values taken in a continuous way. When there is evidence of fouling, instead of using the absolute value of the particle concentration we prefer to filter the data and analyze the value of the fluctuations; this has been done by using a lowpass Butterworth filter of second order [16].

3. Results and discussion

Fig. 1 shows the thermal evolution of the reservoir for the period June–October, 2000. The thermal evolution of the reservoir in summer is highly affected by the withdrawal of water for irrigation, which is taken at 116 m ASL, at 7 m height from the bottom (Fig. 1). Due to the extraction of the hypolimnetic water, the warm, oxygenated and phosphorous depleted epilimnetic water progressively occupies the whole column. As a result, in

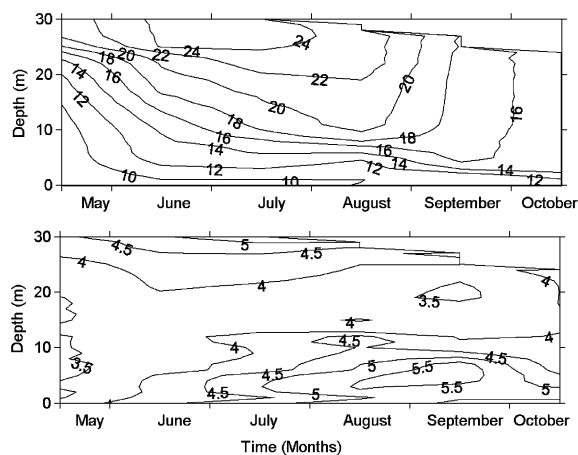


Fig. 1. Top: Isolines of temperature from 15 May to 15 October 2000, at the deepest point in Boadella reservoir. Bottom: Isolines of PNC, in units of particles/mL, at the deepest point in Boadella reservoir; the isolines refer to PNC log-contours.

autumn, the depth of the seasonal thermocline coincides with the depth of the water spill. By mid-November, the whole water column is nearly homogeneous, and by the end of the year the stratification has been completely removed, and only a slight stratification remained in the deepest part of the reservoir.

High values for the PNC in the reservoir—together with high values of Chl *a* (data not shown) occur near the surface (Fig. 1) in early mid-summer. Therefore, most of the surface particles can be attributed to the summer phytoplankton bloom. The PNC near the surface decreased as the thermocline deepened. From mid-July to October, the PNC increased at the bottom layer, with values even higher than those found at the surface. Observations under the microscope showed that the phytoplankton bloom was mostly composed of diatoms and green algae. The accumulation of particles close to the bottom of the reservoir, hereafter called the particle boundary layer, also coincides with the main thermocline (Fig. 1). Like the thermal stratification, this particle boundary layer was completely destroyed by the end of the year.

Fig. 2A shows the size class distribution of particles at different depths, on 28 September. As can be seen from the particle size distribution obtained at 4 and 7 m from the bottom, the particle distribution changes in the particle boundary layer. Here the PVC increases and four peaks in the distribution pattern can be observed. Observation under the microscope showed that the smallest particles ($d < 3 \mu\text{m}$) corresponded to inorganic particles and decomposed organic particles. The peaks of particles centered at $d = 5$ and $d = 15 \mu\text{m}$ can be

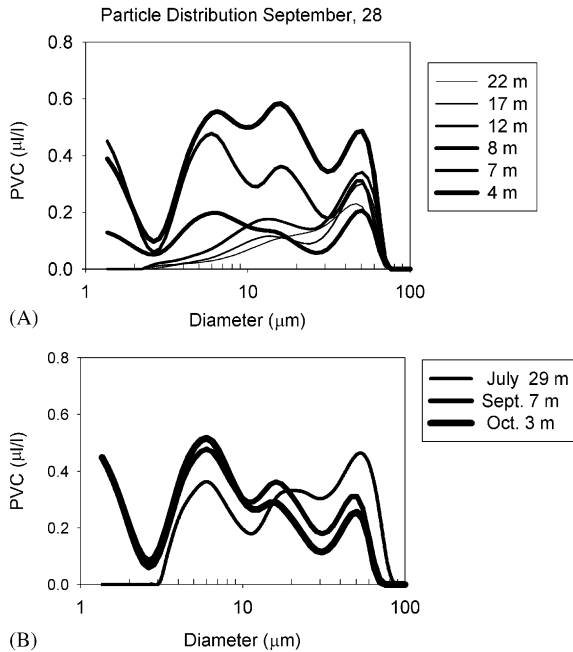


Fig. 2. (A) Particle size distribution—in units of PVC ($\mu\text{L/L}$)—at different depths in Boadella reservoir on 28 September 2000. (B) Comparison between particle size distributions at different dates during the year 2000, at selected depths. Note that the depth is measured from the bottom of the reservoir.

attributed to dead cells of diatoms and green algae, respectively, which sedimented from the surface layers. Particles with diameters between 30 and 100 μm were composed of a mixture of aggregates of inorganic particles, colonies of phytoplankton, zooplankton, detritus, etc. (Fig. 3). The particle size distribution on 7 July at 29 m from the bottom and within the phytoplankton bloom, can be compared with the particle sizes distribution in the boundary layer in September, at 7 m from the bottom, and in October, at 3 m from the bottom (Fig. 2B). The similarity between these distributions indicates that the particle boundary layer is, to a great extent, formed due to the sedimentation of cells from the phytoplankton surface bloom.

Fig. 4 shows the temperature and the PVC profiles for the particles with $d < 3 \mu\text{m}$ and particles with diameters between 30 and 100 μm from 28 September until 17 October 2000. Between these two dates, continuous measurements of the temperature and the size of the particles were carried out. Fig. 4 also shows the position where the LISST-100 was moored (at 8 m from the bottom). On 28 September, the smallest particles ($d < 3 \mu\text{m}$) were concentrated in the thermocline, with its main peak at 6 m from the bottom (Fig. 4A). Although all the particles with diameter $d < 30 \mu\text{m}$ have their maximum concentration in the thermocline, for the sake of clarity in Fig. 4 we have only shown the PVC of

the smallest particles ($d < 3 \mu\text{m}$). The settling velocity for a particle with diameter 3 μm and density 2500 kg/m^3 estimated from Stoke's law is in the order of 0.25 m/d. This low velocity and its reduction due to the enhanced drag caused by the difference in density [17] may account for the entrapment of the smallest particles in the thermocline. The largest particles show a very different pattern. On 28 September (Fig. 4B), most of these particles were in the first 15 m of the water column. The PVC is nearly constant ($\sim 2 \mu\text{L/L}$) because of the water mixing. Between 28 September and 17 October, the thermocline deepened 2–3 m and the epilimnetic water cooled 4°C (at a rate of $\sim 0.2^\circ\text{C/d}$). A fraction of the particles forming the boundary layer was resuspended and the peak of the small particles deepened by the same amount as the thermocline (Fig. 4C). Some of the largest particles have also been removed from the epilimnetic waters through settling and the PVC in the epilimnion has been reduced to 0.5 $\mu\text{L/L}$ approx. (Fig. 4D). The resulting peak due to the sedimentation of the particles was found at 5 m from the bottom.

The continuous temperature measurements show that the reservoir is destratifying as time increases (Fig. 5A). As a consequence, the PVC for the smallest particles measured by the LISST-100 was found to decrease by one order of magnitude, from time ~ 130 h to time ~ 144 h (Fig. 5B). Note that the y-scale for the first 192 h, in Fig. 5B is on the left, while the scale on the right refers to the remaining time. In Fig. 5A can be clearly appreciated an oscillation of the temperatures T_2 and T_3 of period ~ 13 h, beginning at 96 h. As the wind velocity—measured at a meteorological station close to the reservoir—and the temperature (T_3) were found in phase (Fig. 6), the temperature oscillation was considered to be forced by the wind. During this episode, the wind was blowing from the North and reached maximum values of 10 m/s. Also, it is interesting to note that the correlation between the PVC of the small particles is out of phase with the temperature T_3 . This can be understood by taking into account that the measurements of the LISST-100 and T_3 were taken at the same depth of 8 m from the bottom, just above the main peak of small particles (Fig. 4A). A decrease in T_3 meant that water from the boundary layer upwelled and therefore the vertical transport of small particles was enhanced. As a result, the PVC for the smallest particles ($d < 3 \mu\text{m}$) decreased by one order of magnitude (Fig. 5B). A similar oscillation pattern to one described at time ~ 96 h occurred between time ~ 192 h and ~ 240 h (Fig. 5A and B). Although one may speculate that the two sharp peaks of PVC in this period (Fig. 5B) could partly be due to fouling, this effect would occur for a very short time, since the time series soon dropped to a regular pattern. The same can be said for the other peaks in the rest of the time series. Particles with $d < 30 \mu\text{m}$

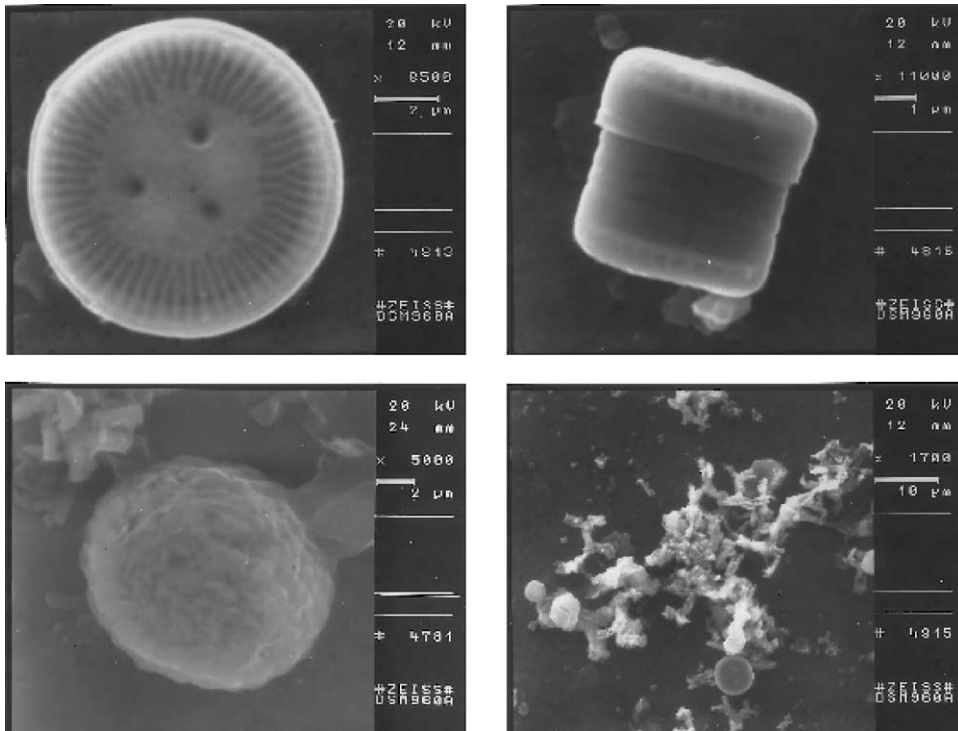


Fig. 3. Scanning electron microscope photographs of the particles in Boadella reservoir. The two scans on top correspond to diatoms. Bottom left scan is green algae. Bottom right scan is a mixture of different organic and inorganic particles; on bottom of the image a diatom can be appreciated.

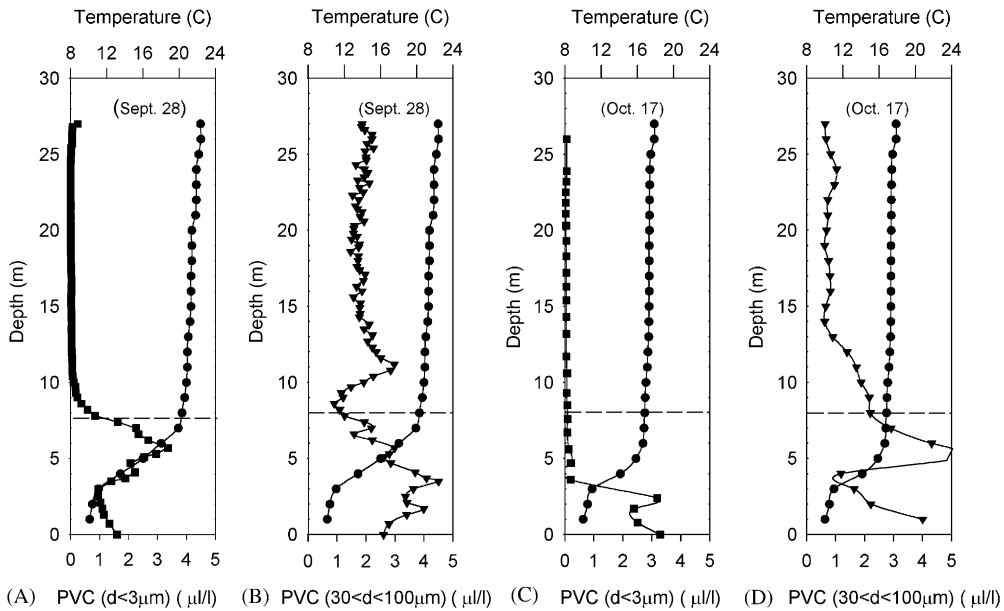


Fig. 4. Vertical profiles of temperature (A) and PVC (B) on 28 September 2000 and on 17 October 2000 (C and D). Circles refer to temperature, squares to particles with diameter $d < 3 \mu\text{m}$, and triangles to particles with diameter between 30 and $100 \mu\text{m}$. Discontinuous lines at 8 m show the position where the LISST-100 was moored.

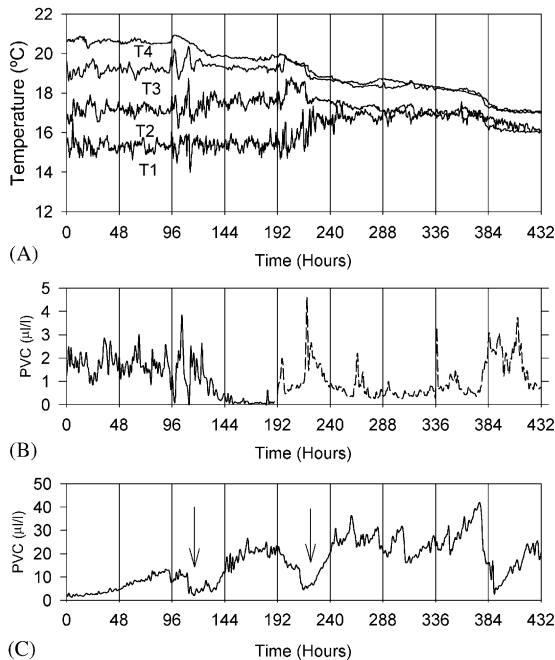


Fig. 5. (A) Time series of temperature from 28 September 2000. The depths at which the temperatures T_1 , T_2 , T_3 and T_4 were taken are 6, 7, 8 and 12 m, respectively, from the bottom (see Fig. 4). (B) Time series of PVC ($\mu\text{L/L}$) for particles with diameter $d < 3 \mu\text{m}$. Notice that until the hour 192 we use the scale on the left hand side, and after the hour 192, the scale on the right hand side. (C) Time series of PVC ($\mu\text{L/L}$) for particles with diameter between 30 and $100 \mu\text{m}$. The arrows indicate when fouling took place (see the text).

(data not shown), behave in a way which is similar to particles with $d < 3 \mu\text{m}$.

The time series of particles with a diameter range of 30– $100 \mu\text{m}$ (Fig. 5C) show high PVC values which are unrealistic when compared with the results obtained with the discrete particle profiles (Fig. 4B and D). Discrete particle profiles showed maximum concentration values of $5 \mu\text{L/L}$, while continuous concentration profiles showed maximum concentration values of $40 \mu\text{L/L}$. As pointed out in the Section 2, the unrealistic measurements are associated with fouling, which affects the instrument optics. During the first 96 h, the PVC increased exponentially until eventually, with the onset of the oscillation described in the previous paragraph, the optical window was cleaned and the concentration dropped to normal values (see the first arrow in Fig. 5C). The cleaning of the window occurred because of the upwelled water, as explained in the previous paragraph. A similar pattern can be observed between the hours 192 and 240 (see the second arrow in Fig. 5C). Because of the fouling effect, from here onward, we will analyze our results by using the concentration fluctua-

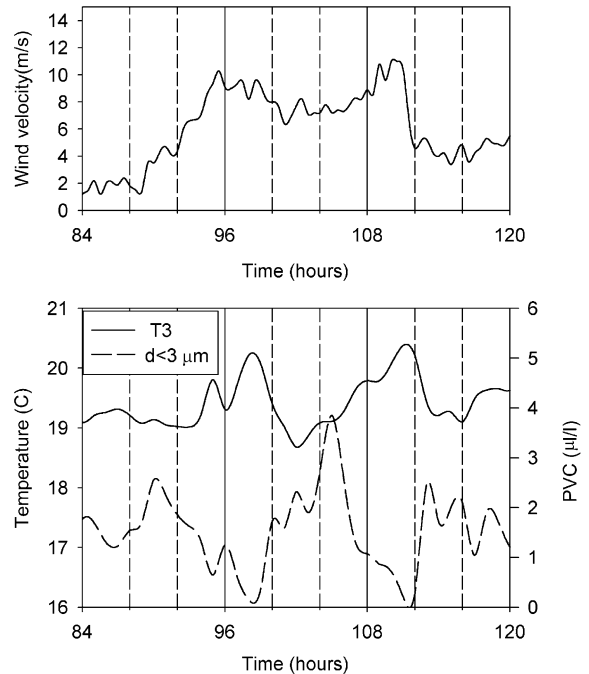


Fig. 6. Above: Wind velocity measured at a meteorological station close to Boadella reservoir. Below: Temperature (T_3) and PVC for the particles with diameter $d < 3 \mu\text{m}$ for the same period of time as that of the wind data.

tions of a given size class, rather than their absolute values.

Fig. 7A–C shows the fluctuations in temperature and in PVC, for the particles with $d < 3 \mu\text{m}$ and particles with diameters between 30 and $100 \mu\text{m}$, during the studied period. At the beginning of this period the peak for particles with $d < 3 \mu\text{m}$ and the thermocline level, were within a short distance of the LISST-100 position (Fig. 4A). However, the peak of PVC for the particles with diameters between 30 and $100 \mu\text{m}$ was found far from the LISST-100. During the first 144 h, the temperature and the small particles fluctuate to a greater extent than during the rest of the period (Fig. 7A and B). After the first 144 h the temperature and the particle profiles approached the ones measured at the end of the period (Fig. 4C) and therefore the LISST-100 was found far from the thermocline and the concentration peak for the small particles. Therefore the fluctuations decreased considerably. However, the role played by the largest particles was the opposite. After the first 144 h, the peak of these particles was close to the LISST-100 (Fig. 4D) and the fluctuations were larger (Fig. 7C)

The correlation coefficient between the temperature (T_3) and the PVC time series for the different particle sizes is presented in Table 1. As the temperature T_3 and

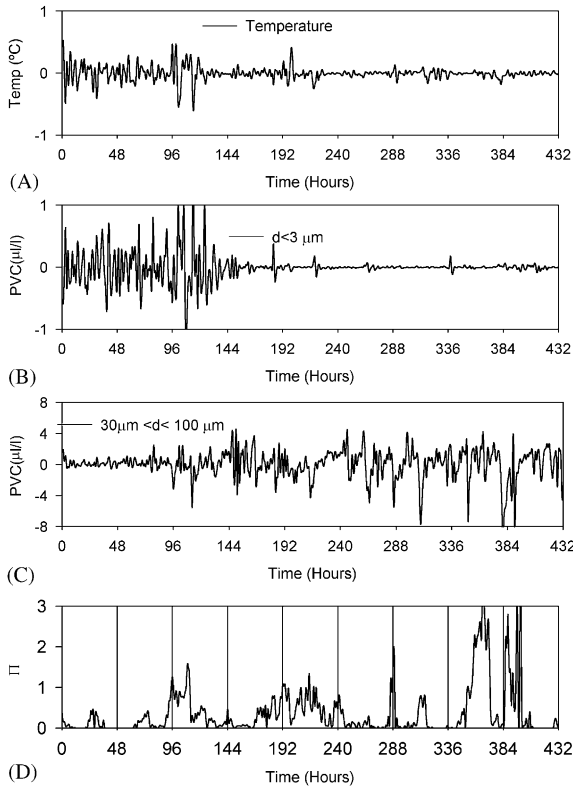


Fig. 7. Time fluctuations series of temperature (A), PVC for particles with diameter $d < 3 \mu\text{m}$ (B), PVC for particles with diameter between 30 and $100 \mu\text{m}$ (C) and time series of the non-dimensional number Π (see Eq. (1) in the text).

Table 1

Correlation coefficient between the temperature T_3 and PVC time series for: A—First 144 h of the experiment and B: from 240 to 432 h

	A	B
$d < 3 \mu\text{m}$	-0.62	-0.36
$3 \mu\text{m} < d < 10 \mu\text{m}$	-0.48	-0.37
$10 \mu\text{m} < d < 30 \mu\text{m}$	-0.25	0.02
$30 \mu\text{m} < d < 100 \mu\text{m}$	-0.19	0.07

PVC were measured at the same depth, a high correlation would mean a dynamic similarity between the water and particles. In order to calculate the correlation we divided the time series into two periods. Period A corresponds to the first 144 h and period B corresponds to 240–432 h. In period A, internal waves were dominant at the depth where the LISST-100 was measuring and there was a good negative correlation between the time series of temperature and small particles ($d < 3 \mu\text{m}$). The correlation was found to decrease with the particle size. The negative sign is due

to the fact that when the temperature decreased, an upwelling of water from the particle boundary layer took place. The higher size particles followed a completely different pattern. In period A, the fluctuations of these particles were small, but in period B they were enhanced. This can be understood by taking into account that these particles, at the beginning of period A (Fig. 4B) were mostly at the surface layers of the lake, at a considerable distance from the LISST-100. The instrument detected the largest particles when they settled through the thermocline. During period A the thermal gradient still prevented the fluctuations from increasing; however, in period B mixing was enhanced and all these particles fluctuated to a larger extent. From hour 144 to the end (period B), convection became dominant and there was not such a good correlation between temperature and the particle measurements.

Based on the above findings, the problem of resuspension of particles at the bottom boundary layer ought to be governed by the stress across the top interface due to internal motions and the strength of the stratification of the bottom boundary layer. We can define the non-dimensional number

$$\Pi = \frac{\rho u_*^2 L}{\Delta \rho g h^2} \quad (1)$$

where ρ is a reference water density, u_* is the water shear velocity, L is a horizontal length scale, $\Delta \rho$ is the density difference through the interface, g is the gravity acceleration, h is a vertical length scale for the resuspension. We calculated u_* from the wind velocity, U , measured at the meteorological station of Agullana ($u_* = (C_D \rho_a / \rho)^{1/2} U$ where the drag coefficient $C_D = 1.3 \times 10^{-3}$, and the air density $\rho_a = 1.2 \text{ kg/m}^3$). For the horizontal length scale we use the wind fetch $L = 1.5 \text{ km}$. $\Delta \rho$ is calculated from the difference in density between T_1 and T_3 (Fig. 5). For the vertical length scale we used the width of the thermocline $h = 5 \text{ m}$. This non-dimensional number is similar to the Wedderburn number [1]; however the Wedderburn number is used as an indicator of the upwelling from the metalimnion into the surface layer. In Fig. 6D the time series of the values of Π is displayed. It can be noticed that the first time that Π was greater than 1, was at around 96 h, during the oscillation that resuspended the small particles (Fig. 4B). From here on, Π was greater than 1 several times. For example, after $t = 336 \text{ h}$ Π reached the largest values. Note the “burst” of particles in Fig. 5B following the high Π values, indicating that particles were resuspended.

4. Conclusions

By using the particle sizer instrument LISST-100 we have measured the evolution of the boundary layer in a

reservoir. The formation of this boundary layer was related to the thermal stratification formed at the bottom of the reservoir due to water withdrawal. LISST-100 provides better estimates of suspended sediment concentration than are possible with previous sensor systems. One of the drawbacks of LISST-100, and in general of all optical sensors, is the fouling of the optical windows. This has to be born in mind when data is analyzed. This instrument provides a quick way to identify different populations of phytoplankton in lakes, if a few observations with the microscope have been carried out previously. Here, for example, populations of diatoms and green algae, with concentration peaks centered at diameters of 5 and 15 μm , were identified as the major components of the summer bloom. After settling, and due to the thermal stratification, these populations remained trapped in the boundary layer. We used a thermistor string moored together with the LISST-100 to characterize all the major features of the dynamics of particles in the reservoir during a certain period. The general picture was as follows: At the beginning of this period (28 September 2000) the small particles ($d < 30 \mu\text{m}$) were trapped in the boundary layer while the largest ones were in the surface layers ($30 \mu\text{m} < d < 100 \mu\text{m}$). By the end of the period (17 October 2000) the boundary layer was eroded, the small particles were resuspended and most of the big particles settled down. As a measure of the extent of resuspension, we propose the use of the non-dimensional number Π (see Eq. (1)). When $\Pi > 1$ resuspension was enhanced.

Acknowledgements

Financial support was provided by the Spanish Ministry of Science and Technology (MCYT) under the project REN2000-0639 HID. Also the Catalan Agency for the Water (ACA) provided technical support as well as the boat used in this study.

References

- [1] Imberger J. Characterizing the dynamical regimes of a lake. In: Xavier Casamitjana, editor, Physical processes in natural waters. Universitat de Girona, Spain: Servei de Publicacions, 2001. p. 77–92.
- [2] Agrawal YC, Traykovski P. Particles in the bottom boundary layer: concentration and size dynamics through events. *J Geophys Res* 2001;106(C5):9532–42.
- [3] Gloor M, Wüest A, Imboden DM. Dynamics of mixed bottom boundary layers and its implications for diapycnal transport in a stratified, natural water basin. *J Geophys Res* 2000;105(C4):8629–46.
- [4] MacIntyre S, Flynn KM, Jellison R, Romero J. Boundary mixing and nutrient fluxes in Mono Lake (California). *Limnol Oceanogr* 1999;44(3):512–9.
- [5] Wieland E, Lieneman P, Bollhalder S, Lück A, Santschi PH. Composition and transport of settling particles in Lake Zurich: relative importance of vertical and lateral pathways. *Aquat Sci* 2001;63:123–49.
- [6] Dickey TD, Chang GC, Agrawal YC, Williams AJ, Hill PS. Sediment resuspension in the wakes of Hurricanes Edouard and Hortense. *Geophys Res Lett* 1998;25(18):3533–6.
- [7] Mikkelsen OA, Pejrup M. The use of a LISST-100 laser particle sizer for in situ estimates of floc size, density and settling velocity. *Geo-Mar Lett* 2001;20:187–95.
- [8] Granata TC, Serra T, Colomer J, Casamitjana X, Duarte CM, Garcia E. Flow and particle distributions in a nearshore seagrass meadow before and after a storm. *Mar Ecol Progr ser* 2001;298:95–106.
- [9] Alldredge AL, Gotschalk C. In situ settling behaviour of marine snow. *Limnol Oceanogr* 1988;33:339–51.
- [10] Knowles SC, Wells JJ. In situ aggregate analysis camera (ISAAC): a quantitative tool for analyzing fine grained suspended material. *Limnol Oceanogr* 1998;43:1954–62.
- [11] Ridd P, Day G, Thomas S, Harradence J, Fox D, Bunt J, Renagi O, Jago C. Measurement of sediment deposition rates using an optical backscatter sensor. *Estuarine Coastal Shelf Sci* 2001;52:155–63.
- [12] Lampitt RS, Hillier WR, Challenor PG. Seasonal and diel variation in the open concentration of marine snow aggregates. *Nature* 1993;362:737–9.
- [13] Bale AJ, Morris AW. In situ measurements of particle size in estuarine waters. *Estuarine Coastal Shelf Sci* 1987;24:253–63.
- [14] Agrawal YC, Pottsmith HC. Instruments for particle size and settling velocity observations in sediment transport. *Mar Geol* 2000;168:89–114.
- [15] Jorgensen BB, Kuenen JG, Cohen Y. Microbial transformations of sulfur compounds in a stratified lake (Solar lake, Sinai). *Limnol Oceanogr* 1979;24:799–822.
- [16] Orfanidis SJ. Optimum signal processing. An introduction, 2nd Ed. Englewood Cliffs, NJ: Prentice-Hall, 1996.
- [17] Srdic-Mitrovic AN, Mohamed NA, Fernando HJS. Gravitational settling of particles through density interfaces. *J Fluid Mech* 1999;381:175–98.